

ARMY RESEARCH LABORATORY



Hypervelocity Penetration Impacts in Concrete Targets

by Alexander E. Zielinski and Graham F. Silsby

ARL-TR-2038

September 1999

19991008 065

Approved for public release; distribution is unlimited.

DTIC QUALITY INSPECTED 4

The findings in this report are not to be construed as an official Department of the Army position unless so designated by other authorized documents.

Citation of manufacturer's or trade names does not constitute an official endorsement or approval of the use thereof.

Destroy this report when it is no longer needed. Do not return it to the originator.

Army Research Laboratory

Aberdeen Proving Ground, MD 21005-5066

ARL-TR-2038

September 1999

Hypervelocity Penetration Impacts in Concrete Targets

Alexander E. Zielinski and Graham F. Silsby
Weapons and Materials Research Directorate, ARL

Abstract

Electromagnetic launch offers the acceleration of projectiles to velocities larger than those provided by conventional chemical guns. The potential effect of large-impact energies on targets other than armor has great promise for replacing high-explosive (HE) payloads with inert hypervelocity rounds. A double-layer reinforced concrete (DLRC) wall, which has been reduced in scale, was the target. Tests were conducted with aluminum cylindrical projectiles launched at velocities up to $2,223\text{ m/s}$ for a 46-g slug and $1,462\text{ m/s}$ for a 92-g slug. Data concerning the muzzle velocity and target damage were recorded. Additionally, the residual penetration into an aluminum plate was recorded. The diameter of the hole in the concrete target increased from 100 mm to the full lateral dimension of the target (450 mm), with increasing impact velocity. The data suggest that there was increased damage to the concrete target by an impact from a hypervelocity slug, as compared to an equal-energy impact at ordnance velocity. Although residual penetration was minimal with the smaller projectile, additional engineering and tests with a bimetallic slug may be able to balance terminal performance and further demonstrate the utility of hypervelocity.

REPORT DOCUMENTATION PAGE			<i>Form Approved</i> OMB No. 0704-0188	
Public reporting burden for this collection of information is estimated to average 1 hour per response, including the time for reviewing instructions, searching existing data sources, gathering and maintaining the data needed, and completing and reviewing the collection of information. Send comments regarding this burden estimate or any other aspect of this collection of information, including suggestions for reducing this burden, to Washington Headquarters Services, Directorate for Information Operations and Reports, 1215 Jefferson Davis Highway, Suite 1204, Arlington, VA 22202-4302, and to the Office of Management and Budget, Paperwork Reduction Project (0704-0188), Washington, DC 20503.				
1. AGENCY USE ONLY (Leave blank)	2. REPORT DATE September 1999	3. REPORT TYPE AND DATES COVERED Final, August-December 1998		
4. TITLE AND SUBTITLE Hypervelocity Penetration Impacts in Concrete Targets			5. FUNDING NUMBERS 1L162618AH80	
6. AUTHOR(S) Alexander E. Zielinski and Graham F. Silsby				
7. PERFORMING ORGANIZATION NAME(S) AND ADDRESS(ES) U.S. Army Research Laboratory ATTN: AMSRL-WM-BC Aberdeen Proving Ground, MD 21005-5066			8. PERFORMING ORGANIZATION REPORT NUMBER ARL-TR-2038	
9. SPONSORING/MONITORING AGENCY NAMES(S) AND ADDRESS(ES)			10. SPONSORING/MONITORING AGENCY REPORT NUMBER	
11. SUPPLEMENTARY NOTES				
12a. DISTRIBUTION/AVAILABILITY STATEMENT Approved for public release; distribution is unlimited.			12b. DISTRIBUTION CODE	
13. ABSTRACT (Maximum 200 words) <p>Electromagnetic launch offers the acceleration of projectiles to velocities larger than those provided by conventional chemical guns. The potential effect of large-impact energies on targets other than armor has great promise for replacing high-explosive (HE) payloads with inert hypervelocity rounds. A double-layer reinforced concrete (DLRC) wall, which has been reduced in scale, was the target. Tests were conducted with aluminum cylindrical projectiles launched at velocities up to 2,223 m/s for a 46-g slug and 1,462 m/s for a 92-g slug. Data concerning the muzzle velocity and target damage were recorded. Additionally, the residual penetration into an aluminum plate was recorded. The diameter of the hole in the concrete target increased from 100 mm to the full lateral dimension of the target (450 mm), with increasing impact velocity. The data suggest that there was increased damage to the concrete target by an impact from a hypervelocity slug, as compared to an equal-energy impact at ordnance velocity. Although residual penetration was minimal with the smaller projectile, additional engineering and tests with a bimetallic slug may be able to balance terminal performance and further demonstrate the utility of hypervelocity.</p>				
14. SUBJECT TERMS hypervelocity, concrete, penetration			15. NUMBER OF PAGES 36	
			16. PRICE CODE	
17. SECURITY CLASSIFICATION OF REPORT UNCLASSIFIED	18. SECURITY CLASSIFICATION OF THIS PAGE UNCLASSIFIED	19. SECURITY CLASSIFICATION OF ABSTRACT UNCLASSIFIED	20. LIMITATION OF ABSTRACT UL	

INTENTIONALLY LEFT BLANK.

ACKNOWLEDGMENTS

Dr. Ed Schmidt, manager for the U.S. Army's Electric Gun Program, supported this effort. Mr. Ron Henry, U.S. Army Research Laboratory (ARL), Survivability/Lethality Analysis Directorate (SLAD), provided helpful discussions on target selection. The fabrication of the concrete targets was ably conducted by Mr. Ronnie Bowman and Mr. Steve Horn of Davis Concrete, Aberdeen, MD. A special thanks is offered to Mr. Jerry Davis and Mr. John Wethersby, Waterways Experiment Station (WES), for technical guidance. Additionally, sincere appreciation is further extended to Mr. Jerry Davis for providing the reduced-scale concrete-reinforcement bars used in the tests. Mr. Brendan Patton and Mr. Donald "Mac" McClellan, ARL, expeditiously provided test support. Finally, Dr. Peter Plostins, ARL, provided a careful technical review.

INTENTIONALLY LEFT BLANK.

Table of Contents

	<u>Page</u>
Report Documentation Page	iii
Acknowledgments	v
List of Figures	ix
List of Tables	xi
1. Introduction	1
2. Target	2
3. Propulsion and Launch Package System	7
4. Experiment	12
5. Results	16
6. Summary, Conclusions, and Recommendations	21
7. References	23
Appendix: Interior Ballistic Summary	25
Distribution List	29

INTENTIONALLY LEFT BLANK.

List of Figures

<u>Figure</u>	<u>Page</u>
1. Photograph of One Layer of Reinforcement During Assembly.....	4
2. Target Form With Two Layers of Reinforcement Installed.....	5
3. Solid Propellant Launcher	7
4. Predicted Velocity for 50-g Inbore Mass Using 7-P M30 Propellant.....	8
5. Predicted Velocity for the Optimum M30 and Available M2 Propellants.....	10
6. Photograph of Short-Slug Launch Package (58 g Total).....	11
7. Photograph of the Target Setup.....	13
8. Typical Measured Case Mouth Pressure as a Function of Time.....	13
9. Measured and Calculated Maximum Case Mouth Pressure.....	14
10. Measured and Calculated Velocity.....	14
11. Typical X-ray Images: Muzzle (Left) and ~ 1 m Downrange (Right).....	15
12. Images From High-Speed Film During Impact (2,143 m/s).....	16
13. Measured Normalized Penetration as a Function of Impact Velocity.....	17
14. Illustration of Increasing Impact Velocity on the DLRC Target.....	18

15. Mass Loss as a Function of Impact Velocity..... 19

16. Residual Penetration as a Function of Impact Velocity..... 19

17. Illustration of Impacts for Equal Impact Energies: 86 kJ (Top) and
100 kJ (Bottom).....20

18. Hole Diameter for Equal Impact Energies..... 21

List of Tables

<u>Table</u>	<u>Page</u>
1. Summary of M830A2 Information.....	2
2. Concrete Ingredients	5
3. Concrete Test Results.....	6
4. Launch Package Component Weights.....	11
A-1. Interior Ballistic Summary.....	27

INTENTIONALLY LEFT BLANK.

1. INTRODUCTION

Electromagnetic launchers offer the promise of delivering a substantial amount of energy on a target due to no inherent upper limit on launch velocity. However, it is unclear as to the relative value of this increase in energy. The energy per unit mass for an impact at $3,000\text{ m/s}$ is roughly equal to the heat of explosion for a high explosive (HE) ($5,000\text{ J/g}$). In only the simplest hypervelocity projectile-target interactions (e.g., those of shaped-charge jets and long-rod penetrators attacking armor targets) can the outcomes be predicted with a fair degree of confidence. Most military targets are more complex, as, for example, the composite construction of a steel-reinforced concrete wall. For such targets, modeling hypervelocity perforation is problematic at best. However, if a hypervelocity round has merit against a complex target, then perhaps a HE payload as a lethal mechanism could be replaced with an inert payload. Fewer explosives on the battlefield could significantly simplify logistics.

A typical military target that might be encountered in an urban environment was selected [1]. The details for the target considered in this report can be found in the literature [2]. The full-scale target was a double-layer reinforced concrete (DLRC) wall, 8 in thick (203 mm). Other types of targets were available; however, the DLRC wall was amenable to scaling [3].

Hypervelocity impact data were generated by the use of a high-performance solid propellant laboratory gun. Tests were conducted at velocities up to $2,223\text{ m/s}$ for a 46-g slug and $1,462\text{ m/s}$ for a 92-g slug. Impact results were compared for the 46-g and 92-g slugs as a function of impact velocity. Impacts of the 46-g and 92-g slugs at equal impact energies are also discussed. Damage to the DLRC target was the primary measure of effectiveness. Of secondary concern was the nature of the debris projected behind the target. To explore this issue, the concrete was followed by an air space sufficient to allow fragmented debris to disperse and impact an aluminum plate. Any deep penetration of the aluminum plate would suggest the presence of unconsumed penetrator material.

This report is organized as follows. Section 2 provides a description of the DLRC target and its construction. In section 3, the propulsion system and launch package are defined. Section 4 contains a discussion of the experiment. In section 5, the experimental results are presented. Finally, the last section contains the summary, conclusions, and recommendations.

2. TARGET

The DLRC target represents a typical structural element that might be found as a bunker wall or part of a building. The dimensions and other particulars were based on customer requirements and data that indicated that concrete target performance could be successfully scaled [3]. The DLRC wall that is used in a bunker could be breached by the M830A2 HE fin-stabilized round. The M830A2 is used in the 120-mm M256 smoothbore cannon. The primary internal component is the chemical-energy warhead composed of Composition-A3 Type-II HE. Additionally, a shaped copper liner, which generates a copious pattern of lethal fragments, is used ahead of the HE to provide for some penetration capability at the target. A summary of the specifications on the M830A2 round is listed in Table 1.

Table 1. Summary of M830A2 Information

Complete Weight (kg)	22.7
Launch Weight (kg)	8.4
Launch Velocity (m/s)	1,410
HE Weight (kg)	0.94

The M830A2 round is launched with 8.3 MJ and retains 5 MJ at 1,600 m downrange. If an electromagnetic railgun launched a 90-mm-diameter aluminum slug that impacted the target at a velocity of 2,200 m/s, a mass of 2.1 kg would be necessary to obtain the same energy capacity as the M830A2. Scaling these requirements linearly down to a bore diameter of 26 mm results in a launch mass of roughly 45 g.

The lateral dimensions of the DLRC wall were determined from the size of the crater generated by HE tests [2]. Using the M830A2 explosive weight (*0.94 kg*) gives a wall height of roughly *1.8 m (4 ft)*. The length of the wall should be at least as great as the height. The scale factor determined from the ratio of the full-scale railgun and the laboratory gun diameters (*3.6*), yielded a concrete target with lateral dimensions *330 mm × 330 mm*. Similar experiments on going at the Waterways Experiment Station (WES) utilized concrete targets with lateral dimensions of *457 mm × 457 mm (18 in × 18 in)* [3]. Therefore, in order to provide some consistency between the two experiments, a DLRC target with lateral dimensions of *457 mm* were selected. Also, the wall thickness of the DLRC target reduced from full-scale was *57 mm (2.25 in)*.

The spacing of the reinforcement bars has been found to scale best as the area of the reinforcement [3]. The reinforcement bar specified in the *8-in-thick (203 mm)* bunker target was *1/2 in* in diameter (*13 mm*), grade-40 (i.e., *40-ksi* yield strength) steel spaced on *11 3/4-in (298 mm)* spacing. The reinforcement bars for the full-scale DLRC target were located *3/4 in (19 mm)* below the exterior surface of the concrete (i.e., clear cover). The scaled value of clear cover was approximately *1/4 in (6 mm)*. The scaled bar diameter was *0.14 in (3.5 mm)*; however, the closest readily available diameter was *0.16 in (4 mm)*. In this size, the bars had a strength of *698 MPa (100 ksi)* but were heat-treated to obtain a strength of *414 MPa (60 ksi)* in order to be more compatible with the full-scale DLRC specifications.

The reinforcement ratio is given as

$$p = \frac{A_s}{bd}, \quad (1)$$

where A_s is the cross-sectional area of the steel reinforcement bar, b is the reinforcement spacing (assumed equal in both directions), and d is the distance from the compression face of the concrete to the further most layer of reinforcement. For the full-scale target, $A_s = 126 \text{ mm}^2 (0.196 \text{ in}^2)$, $b = 298 \text{ mm (11.75 in)}$, and $d = (203 - 19) \text{ mm}$. Using these

values gives $p = 0.0023$. Using the dimensions for the scaled target ($A_s = 12.7 \text{ mm}^2$ [0.0198 in^2], and $d = 50 \text{ mm}$ [2.0 in]) gives 109 mm (4.3 in) for the spacing of the reinforcement bars. A nominal value of $4 \frac{3}{8} \text{ in}$ (111 mm) was selected. The bars were placed in a wooden fixture that kept them aligned and spaced $4 \frac{3}{8} \text{ in}$ apart. Steel wire, 0.89 mm in diameter, was used to join the bars at their intersections to keep the steel array rigid. A photograph of one layer of reinforcement bars during target fabrication is shown in Figure 1.



Figure 1. Photograph of One Layer of Reinforcement During Assembly.

The forms for the concrete targets were fabricated from wood. The wood was sealed with several coats of polyurethane prior to assembly to help retain moisture in the concrete during the curing process. The sides of the form have 6-mm -deep (0.25 in) slots to keep the reinforcement bars in place during the pouring and curing procedures. Shown in Figure 2 is the wooden form for the target with the two layers of reinforcement bar installed.

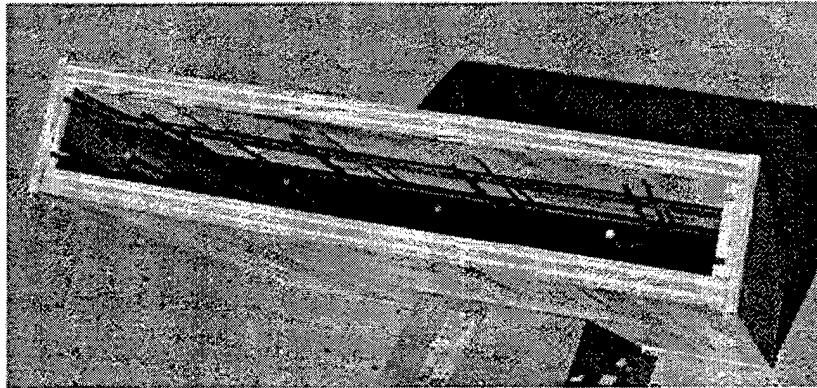


Figure 2. Target Form With Two Layers of Reinforcement Installed.

The concrete was mixed, poured, and tested at a local manufacturing facility. A summary of the ingredients used in the mix is listed in Table 2.

Table 2. Concrete Ingredients

Portland Cement (Type 1)	255.8 kg	564 lb
3/8-in Aggregate	714.4 kg	1,575 lb
Concrete Sand (Dry)	598.3 kg	1,319 lb
Water	124.9 liter	33 gal
Air-Entrainment Admixture	0.13 liter	4.2 oz
Water-Reducing Admixture	0.50 liter	16.9 oz

The compression strength specified for the concrete was 24 MPa ($3,500\text{ psi}$). Appropriate for this scale was $3/8\text{-in}$ pea-gravel aggregate. During pouring, a pneumatic vibrator and mallet tapped the concrete forms and facilitated consolidation. The concrete was moist-cured for the first 7 days. The wooden forms were removed 10 days after the concrete was poured. Small voids (on average 3 mm deep) were present on the surface of the targets. Therefore, a 2-mm layer of quick-setting concrete was applied on the front and rear surfaces of the targets.

Two routine tests were used as quality-assurance measures: the slump test and a test for compressive strength. Just prior to pouring the targets, a sample was poured into a standard open-ended truncated conical metal form. The mix settled for a short time on a

flat surface and the form was removed. The distance that the top of the mound fell was an indication of the water content and relates to the final strength that can be anticipated for the mix. The slump test performed for these targets indicated acceptable water content for a compressive strength of *24 MPa*. The compression test was performed on cylindrical specimens from the initial concrete mix at *10, 17, 24, and 31* days after the targets were poured. These results indicated that the concrete achieved the specified strength. A summary of the results from the slump and compression tests is listed in Table 3. The concrete targets were considered cured on the *24th* day and the impact tests were performed on the *31st* through *33rd* day. Prior to testing, the impact face of the target was painted brown and then marked with white dots, corresponding to the location of the intersection of the reinforcement bars. The markings were repeated for the rear face of the DLRC target; however, yellow paint was used instead of brown to differentiate between the front and rear surfaces.

Table 3. Concrete Test Results

Slump Test	<i>102 mm (4 in)</i>
Compression Tests (post-pour):	
<i>10</i> days	<i>20.8 MPa (3,018 psi)</i>
<i>17</i> days	<i>24.0 MPa (3,487 psi)</i>
<i>24</i> days	<i>24.5 MPa (3,550 psi)</i>
<i>31</i> days	<i>28.0 MPa (4,048 psi)</i>

In addition to the DLRC target, a few slugs were fired into a target that comprised two layers of *2.5-in-thick (63.5-mm)* 7039 aluminum armor plate. These plates were backed by an additional piece of *1-in-thick* rolled homogeneous armor (RHA) plate. The plates were impacted by the slugs at various velocities to develop a baseline penetration vs. velocity relationship for a well-characterized target material. For the shots conducted with the DLRC target, a single *2.5-in-thick* plate was sufficient to record the residual penetration.

3. PROPULSION AND LAUNCH PACKAGE SYSTEM

A 26-mm-diameter smoothbore conventional gun (serial number 5, manufactured by Deep Hole Specialists, Chagrin Falls OH) was used to accelerate the aluminum slugs. This selection was based on prior experience and availability. The barrel was tapped to accept a piezoelectric pressure gauge just beyond the location of the case mouth. The pressure measured at this point does not vary significantly from the breech pressure. The gun was 3 m (10 ft) in length and had a maximum pressure rating of 689 MPa (100 ksi) but had only been operated at 551 MPa (80 ksi). At a maximum breech pressure of 483 MPa (70 ksi), it was difficult to extract the cartridge case from the breech. Above 551 MPa (80 ksi), the cartridge case expanded sufficiently such that it required machining in order to fit into the breech for another shot. The barrel was chambered for the obsolete U.S. 37-mm cartridge case. The bore diameter was reduced to (nominally) 26 mm ahead of the case mouth. A full cartridge case holds 300 g of propellant mass, although it is possible to fit an additional 15 g in the case. A photograph of the launcher with a 37 mm cartridge case in the foreground is shown in Figure 3.

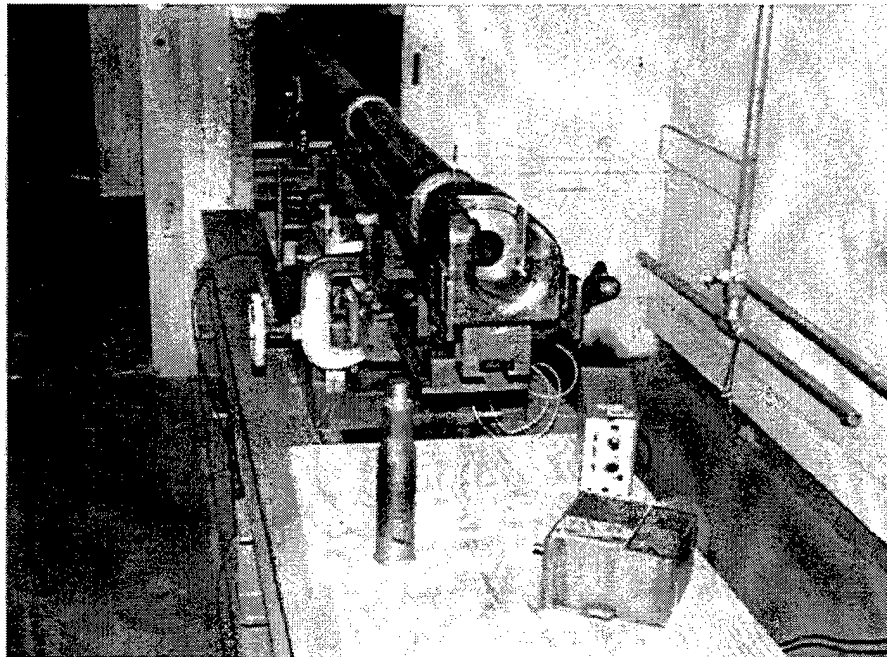


Figure 3. Solid Propellant Launcher.

An interior ballistics code, IBHVG2 [4], was used to provide estimates of the amount of charge (i.e., propellant) necessary to accelerate the launch package to the desired exit velocity. Pressure at the mouth of the cartridge case and exit velocity were predicted from the code. These results were compiled for 2 classes of readily available propellants (single-perforation [1-P] M30 and 7-P M2), 2 launch package masses, and 14 charge masses. In all cases, a rather large in-bore resistance was used for the launch package. It was assumed that an oversized obturator was necessary to properly seal the combustion gases in the excessively worn chamber. The start resistance was 15 MPa and fell to 0 in 10 calibers of travel. The burn-rate data were determined from closed-bomb tests on the M30, 0.46-mm (0.018 in) web propellant and the M2 propellant [5]. Percussive primers, MK22 MOD L70, were readily available and were modeled as 4 g of black powder. A typical plot of the performance results for a 50-g launch package using M30 propellant is shown in Figure 4. Available web sizes for the propellant were considered. Also indicated in the plot are lines of constant breech pressure. The heavy, solid curve indicates the regime where the propellant was not completely consumed at the time of projectile exit. It is desirable to operate the gun above the heavy, solid curve in order to obtain small variability in exit velocity.

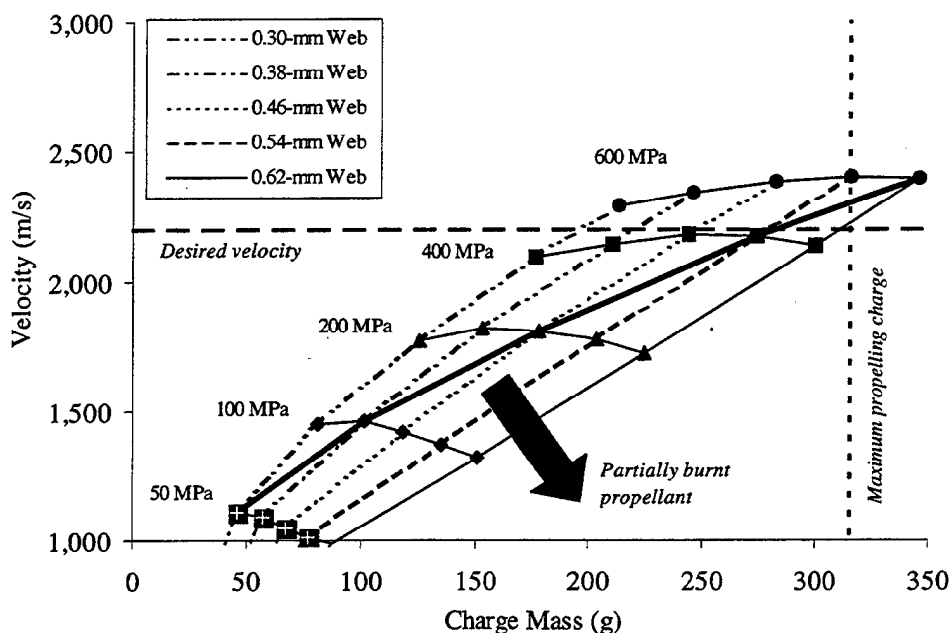


Figure 4. Predicted Velocity for 50-g Inbore Mass Using 7-P M30 Propellant.

From Figure 4, the optimum web size was roughly 0.54 mm (0.022 in) at a peak breech pressure of 600 MPa (87 ksi). However, nearly a full cartridge case of this propellant is required. Slightly less velocity is obtained with the smallest web propellant for significantly less propellant mass. The smaller web propellant is more susceptible to the creation of pressure waves. Significant pressure waves should be avoided as they can in fact destroy the gun system. The 0.46-mm (0.018 in) web propellant can reach the desired velocity ($2,200 \text{ m/s}$) at a reasonable peak breech pressure of roughly 400 MPa (58 ksi) and 244 g of propellant. Propellants with web sizes larger than 0.54 mm (0.022 in) were not capable of meeting the desired velocity, within the constraints of the gun system, owing to the relatively large web size. For these reasons, the best choice of M30 granulation is the 0.46-mm (0.018 in) web size.

The M2 propellant was more energetic than the M30 propellant. A 0.685-mm (0.027 in) web size was readily available. Shown in Figure 5 is a comparison between the optimum M30 and the M2 propellants. The M2 propellant can accelerate the 50-g projectile to the desired velocity with a peak breech pressure of 400 MPa (58 ksi) using 208 g of propellant. While this amount of propellant was less than the amount of M30 propellant for the same level of performance, the M2 propellant had a larger flame temperature and was more erosive than the M30 propellant. Even though both provide the capability for additional amounts of propellant (up to the limit of the case volume, 315 g) in the event that the performance predictions were less than the experimental results, the M30 propellant with 0.46-mm web size was selected for these experiments.

The launch package consisted of an obturator and a carrier fabricated from polypropylux 944 (Westlake Plastic) and a slug fabricated from 7075-T6 aluminum. Polypropylux 944 is a tough and rubbery polypropylene-based plastic. The aluminum slugs were nearly the full diameter of the bore to facilitate the carrier and obturator design. A wall thickness of 1.53 mm (0.060 in) was selected for the polypropylux carrier. Therefore, at a diameter of 24 mm (0.944 in) for the aluminum slug a length of 36.8 mm (1.45 in) yielded the required 45-g mass. The ratio of the length (ℓ) to diameter (d_s) was roughly 1.5 .

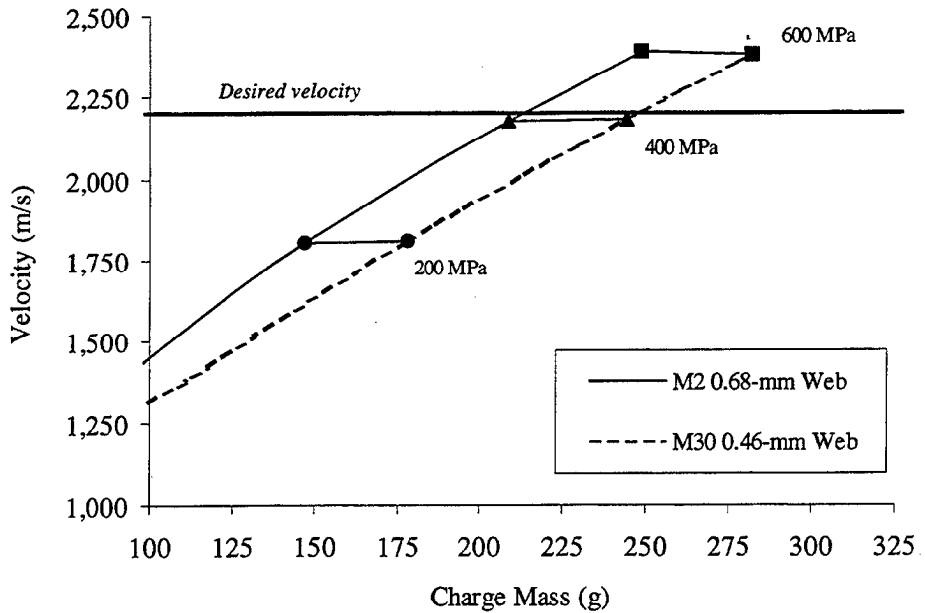


Figure 5. Predicted Velocity for the Optimum M30 and Available M2 Propellants.

The length of the obturator in the axial direction was sized based on minimizing the total mass of the launch package, the shear stress in the obturator, and the fraction of the length of the obturator relative to the total length of the launch package. Based on these considerations, a 14.6-mm-long (0.575 in) obturator was selected. The calculated shear stress on the obturator, at a bore pressure of 551 MPa (80 ksi) is 220 MPa (32 ksi) and exceeds the compressive strength of polypropylux by a factor of 3. The transient response of the material under large high-rate loading conditions and the toughness of the plastic offers some increase in the launch package survivability. The length of the obturator was roughly 28% of the total length of the launch package. A similar analysis was performed for the 90-g aluminum slug. The carriers were cut (the length of the slug) to form four petals. These cuts help the carrier separate from the aluminum slug prior to target impact.

The forward section of the carrier was grooved, 3 mm x 3 mm (1/8 in x 1/8 in) at a minor diameter of 26 mm (1.022 in). The annular grooves provide a volume into which the plastic could flow without generating extreme hydrostatic pressures between the

aluminum slug and the inside surface of the bore. The external diameter of the carrier was 27 mm (1.065 in) and was based on a measured bore diameter of 26.8 mm at the initial location of the launch package in the breech. The obturator diameter was tapered with its smallest diameter equal to 27 mm (1.065 in) to a diameter at the base of the obturator of 27.4 mm (1.080 in). A picture of the completed short-slug launch package is shown in Figure 6.

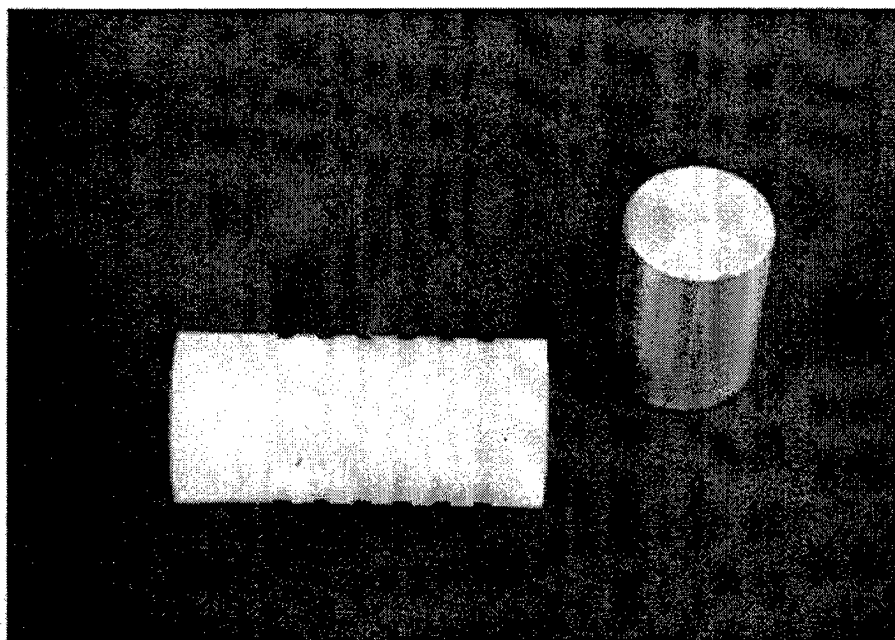


Figure 6. Photograph of Short-Slug Launch Package (58 g Total).

Listed in Table 4 is a summary of the measured mass for the launch package components.

Table 4. Launch Package Component Weights

Aluminum Slug (g)	46.1	92.4
Polypropylux Carrier (g)	11.8	14.9
Total (g)	58.0	107.3

4. EXPERIMENT

The experiment was conducted at the Aerodynamics Experimental Facility located at Aberdeen Proving Ground (APG), MD. The tests were planned such that the shots that subjected the launcher to the most risk (i.e., high pressure, high velocity) were deferred to the end of the experiment. The results from the IBHVG2 simulations were used to estimate the amount of propellant used for each test. For propellant mass less than 250 g, foam sheet was used to line the interior of the case and fill the remaining case volume. Since resources were limited, no attempt was made to correct for differences between the simulation and the experiments.

The DLRC target was held in place on a 1-in-thick steel base. Steel angle was used to hold the DLRC target from the sides and from the front and back. A 1/2-in-thick rubber sheet was placed between the angle and the DLRC target to cushion the target during impact and to reduce the amount of bending in the target. Bending could cause damage to the target not necessarily associated with the penetration of the aluminum cylinder. Located 438 mm (17.25 in) behind the target was a 2.5-in-thick 7039 aluminum plate. This plate was used to assess the residual penetration of the aluminum slug. Additionally, a 1-in-thick RHA plate was used to support the rear of the aluminum plate. A large sheet of cane fiberboard was to be used to record the debris pattern generated behind the DLRC target. However, the material proved insufficient and was not used on subsequent shots. All impact materials were mounted on the steel base that was located 3 m (10 ft) downrange from the muzzle of the gun. A photograph of the target set up is shown in Figure 7.

The launch packages were loaded into the gun using a hydraulic jack. The base of the obturator was seated in the gun 254 mm (10 in) from the rear face of the tube for each shot or a distance of 31.7 mm (1.25 in) between the end of the case and the base of the obturator. The gun was aimed with the use of a bore sight pointed at the center of the DLRC target at a location between the reinforcement bars. The white dots painted on the face of the DLRC target aided in this process.

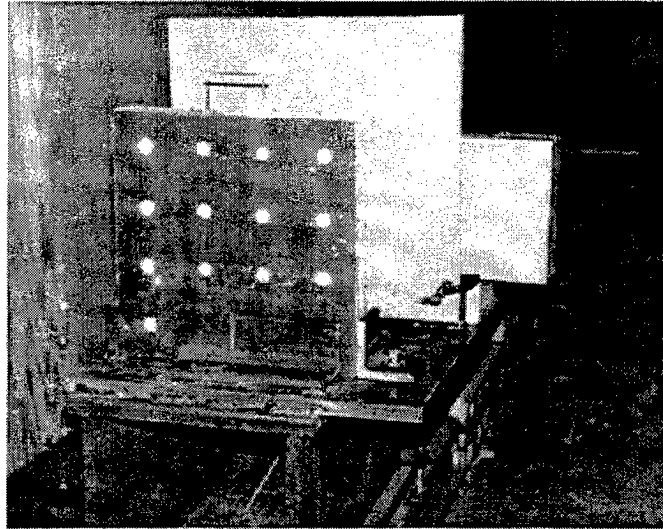


Figure 7. Photograph of the Target Setup.

The pressure at the case mouth was measured using a piezoelectric pressure gauge and charge amplifier. The output of the charge amplifier was stored on a Nicolet model 4094 digital oscilloscope. A typical plot of the pressure is shown in Figure 8. The pressure reaches its maximum value of 588 MPa (85.3 ksi) at 1.12 ms . Thereafter, the propellant continues to burn and the launch package travels downbore, increasing the volume for the expansion of the propellant gas. The slight discontinuities during the rise to peak pressure are indicative of relatively minor pressure waves.

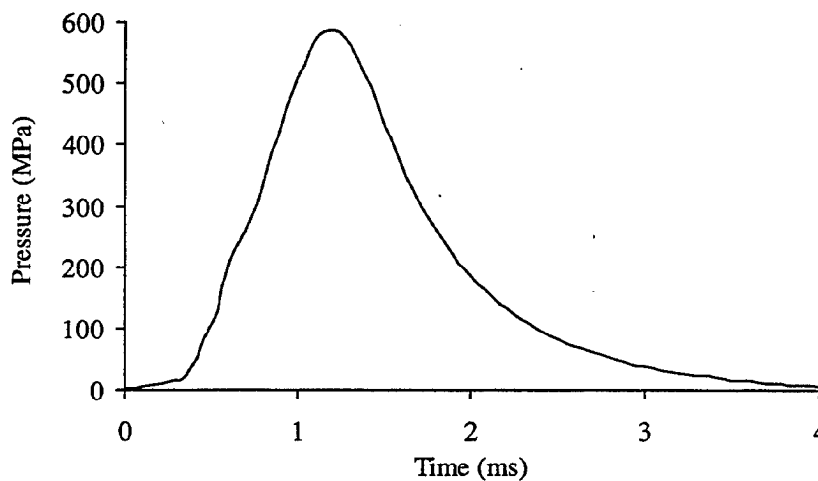


Figure 8. Typical Measured Case Mouth Pressure as a Function of Time.

Shown in Figure 9 is a plot of the maximum case mouth pressure for this test series. The calculations using the IBHVG2 code use the actual launch package masses. It can be seen that the calculations consistently overestimate the measured values. The significant deviation for charge mass less than 200 g between the experimental data, and the theoretical calculations was presumed to occur because not all the propellant was burned during launch package acceleration. In fact, unburned propellant was noticed 1 to 2 m downrange on the x-ray cassette. A similar plot for the launch package velocity is shown in Figure 10.

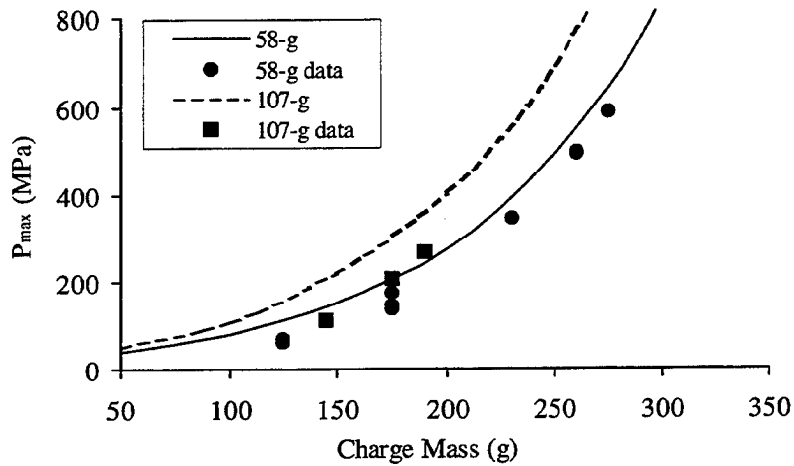


Figure 9. Measured and Calculated Maximum Case Mouth Pressure.

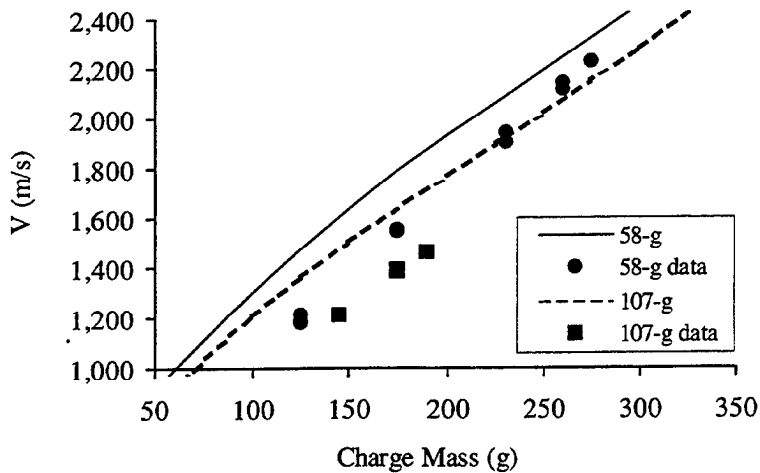


Figure 10. Measured and Calculated Velocity.

The velocity of the slugs was obtained using two flash x-rays, separated by a distance of 0.914 m (3 ft) and located 117 mm from the muzzle of the gun. The flash x-rays were triggered from a signal generated by a pressure transducer located at the muzzle of the gun. Appropriate time delays were calculated from the interior ballistic estimates for the velocity. It was assumed that, after the slug left the gun, there would be very little retardation over the 3-m distance to the DLRC target. The petals of the carrier began to separate at the first x-ray station and were not in the field of view at the second x-ray station. Although the base of the obturator was in close proximity to the aluminum slug, there was no evidence of its impact at the target. Typical x-ray images are shown in Figure 11.

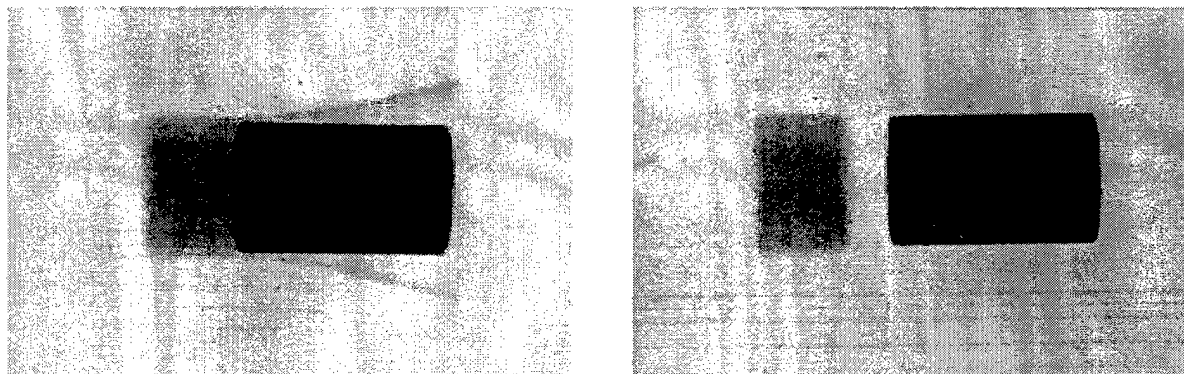


Figure 11. Typical X-ray Images ($1,942\text{ m/s}$): Muzzle (Left) and $\sim 1\text{ m}$ Downrange (Right).

A 16-mm high-speed camera ($4,000\text{ frames/second}$) and a VHS video camera recorded the impact event of the DLRC target. While no quantitative data were obtained from this instrumentation, the images are helpful in diagnosing the behind target effects, as well as any experimental anomalies. A few frames from the high-speed camera film, indicated by the approximate time after impact, are shown in Figure 12. The increased luminosity at $500\text{ }\mu\text{s}$ is due to the impact of the residual penetrator on the aluminum witness plate. The images reveal the amount and extent of debris generated behind the DLRC target.

Additionally, a summary of the interior ballistic data is provided in the Appendix.

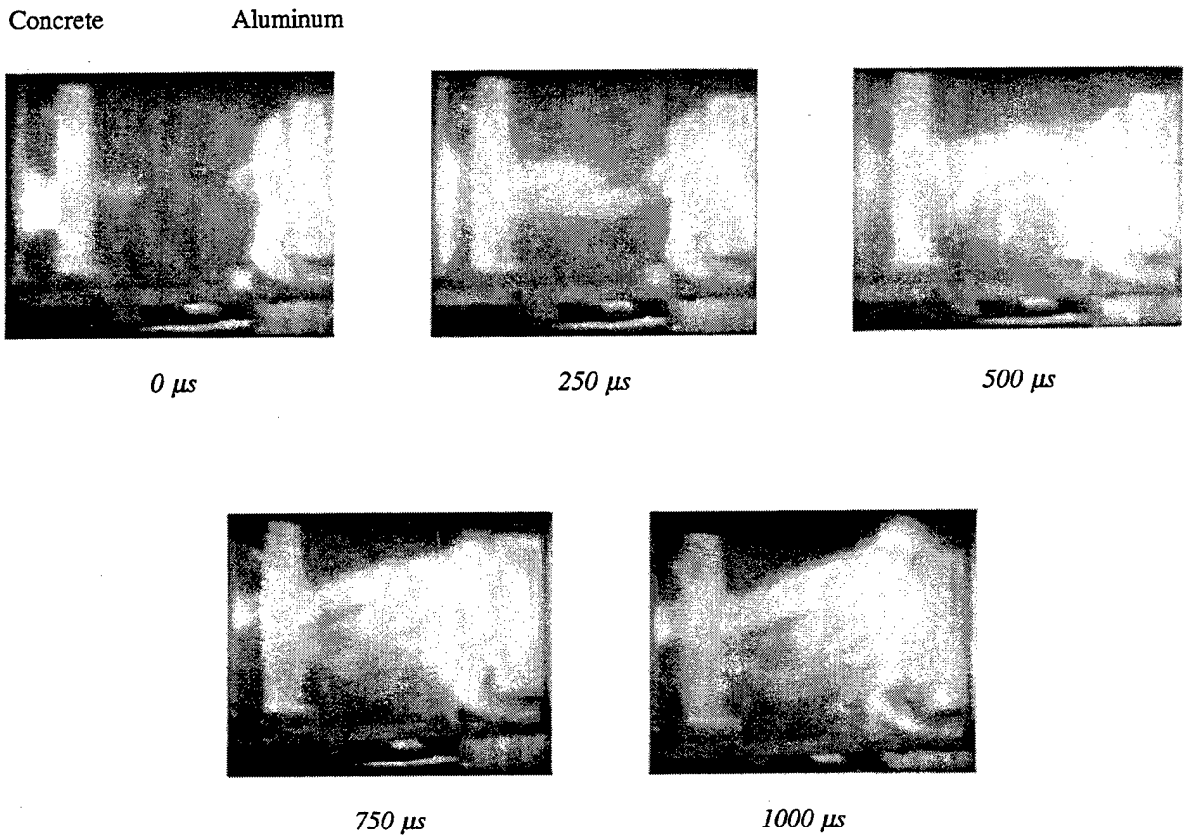


Figure 12. Images From High-Speed Film During Impact (2,143 m/s).

5. RESULTS

Shown in Figure 13 is the measured penetration, P (normalized by the length of the aluminum slug), in the aluminum witness plate in the absence of the DLRC target, as a function of launch velocity. The two projectile masses were considered. This response is typical of a monolithic penetrator impacting a homogeneous target. In the penetration regime, penetration increases readily with increasing impact velocity. At velocities where the impact pressure is well above the material strength (i.e., the hydrodynamic limit), the response is relatively constant. The limit is approximately the square root of the ratio of the penetrator and target densities and is reached approximately at 2,200 m/s.

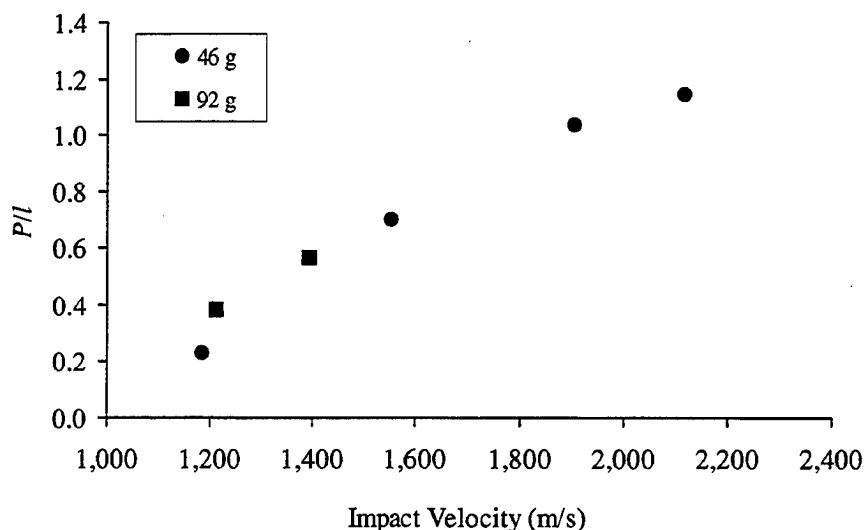


Figure 13. Measured Normalized Penetration as a Function of Impact Velocity.

The effect of increasing impact velocity on the DLRC target is illustrated in Figure 14 for both the front and rear target surfaces. The relative damage to each target can be clearly seen. Note the target support angle at the bottom of each target. The clamp successfully restrained the target without causing it to fracture around the clamp, as would occur if the target were slowly bent backward. The target is held almost entirely by its own inertia during the very short duration of impact; although, some cracks at the impact site extend to the outside edge of the DLRC target even for the lowest velocity. Qualitatively, the extent of target destruction grows with increasing velocity to the point where the concrete matrix along the top edge is missing at the highest velocity, with the attendant loss of one reinforcing bar. There is much more target destruction above the centerline than below. Quantitatively, the damage was assessed by considering the mass removed from the DLRC target, as shown in Figure 15. At ordnance velocity, more than 80% of the target was remaining after the impact. At hypervelocity, one-half of the target was missing. Due to the nature of the target, it was difficult to measure a diameter of the damage to the DLRC target for all but the lowest velocity impacts. The entrance and exit diameters were nearly equal and approached the hole diameter for increasing impact velocities. Despite the irregularly shaped hole, the measurements of the diameter correspond very well to diameters computed from the mass loss and an assumed target density of $5,774 \text{ kg/m}^3$.

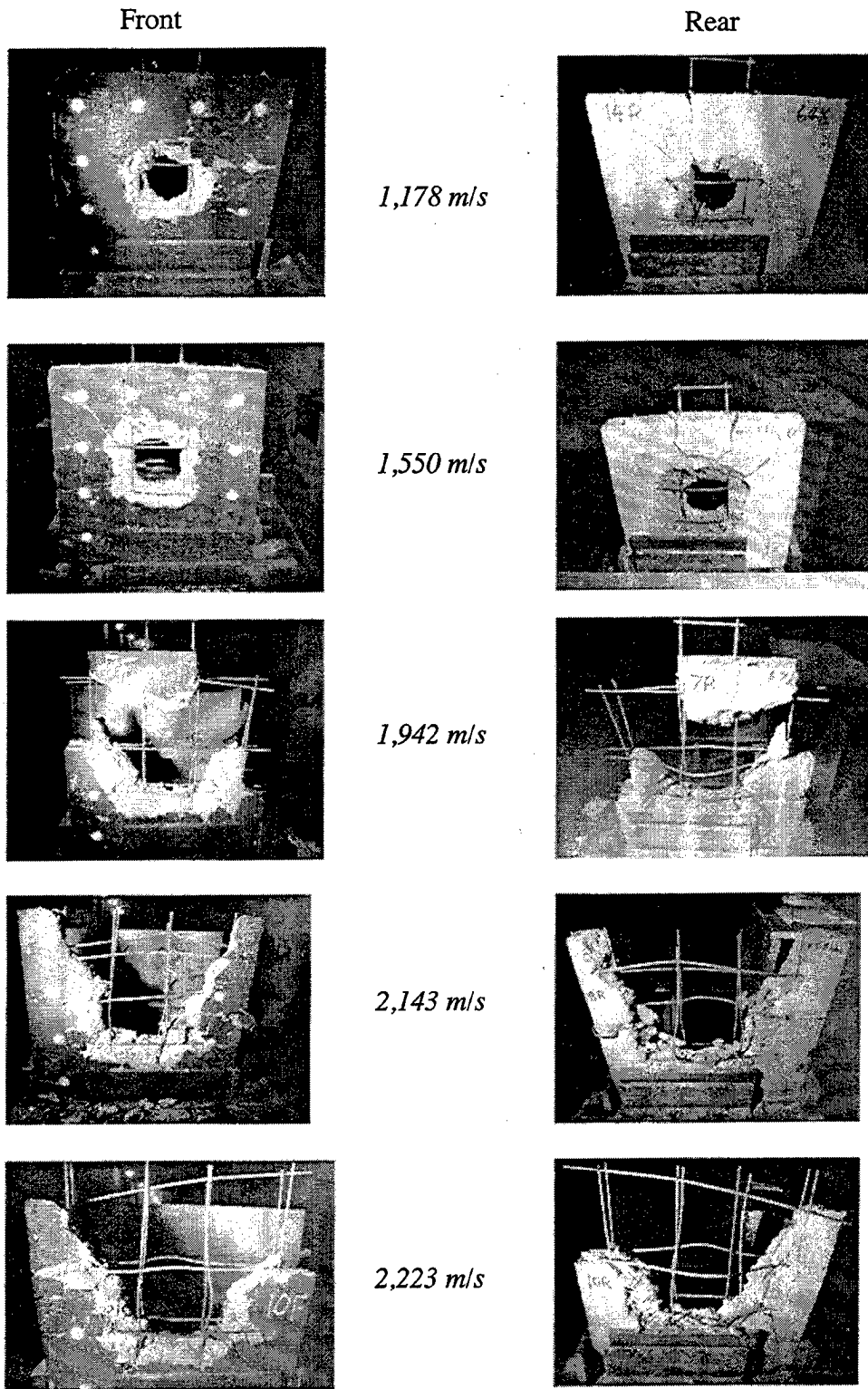


Figure 14. Illustration of Increasing Impact Velocity on the DLRC Target.

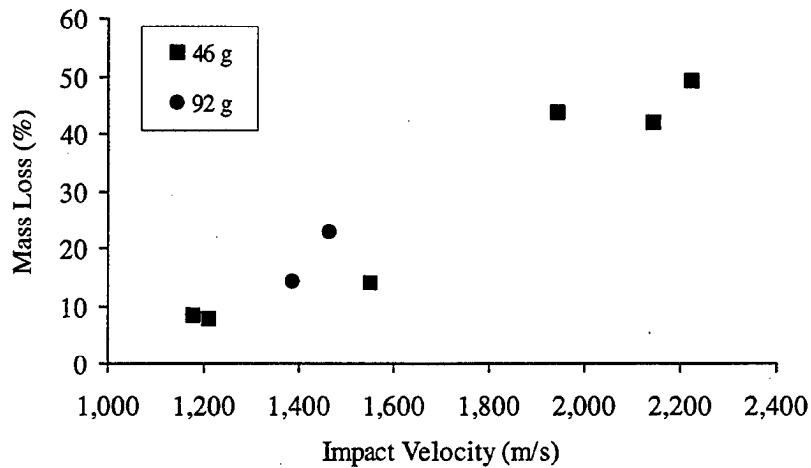


Figure 15. Mass Loss as a Function of Impact Velocity.

Shown in Figure 16 is the measured residual penetration in the aluminum witness plate as a function of impact velocity. The two projectiles were considered. Both projectiles yield approximately constant residual penetration irrespective of the impact velocity. However, the short slug yielded roughly 2 mm of penetration, considerably less than the 15 mm produced by the long slug. The data suggest that the length of the short slug (37 mm) is consumed in the DLRC target. The additional 37 mm provided by the long slug produces the 15 mm of residual penetration. From Figure 13, the velocity of the residual penetrator was estimated to be roughly 1,250 m/s.

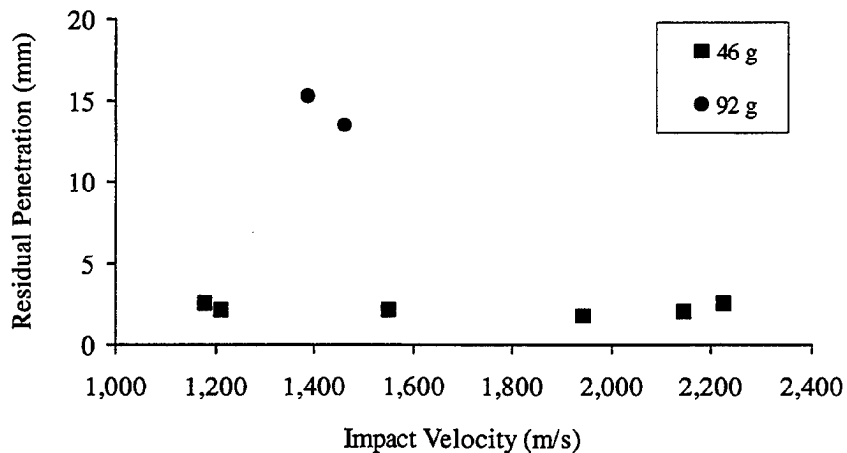


Figure 16. Residual Penetration as a Function of Impact Velocity.

The effect of near equal impact energies for the ordnance and hypervelocity impacts is illustrated in Figure 17. The front surface of the targets is shown. Qualitatively, the images show more damage for the higher velocity impacts than for the lower velocity impacts. Quantitatively, the diameter of the holes was compared in Figure 18. While there appears to be less difference for the higher energy impacts, the diameter of the hole is approaching the lateral dimension of the DLRC target and edge effects may play a significant role in determining the diameter of the hole.

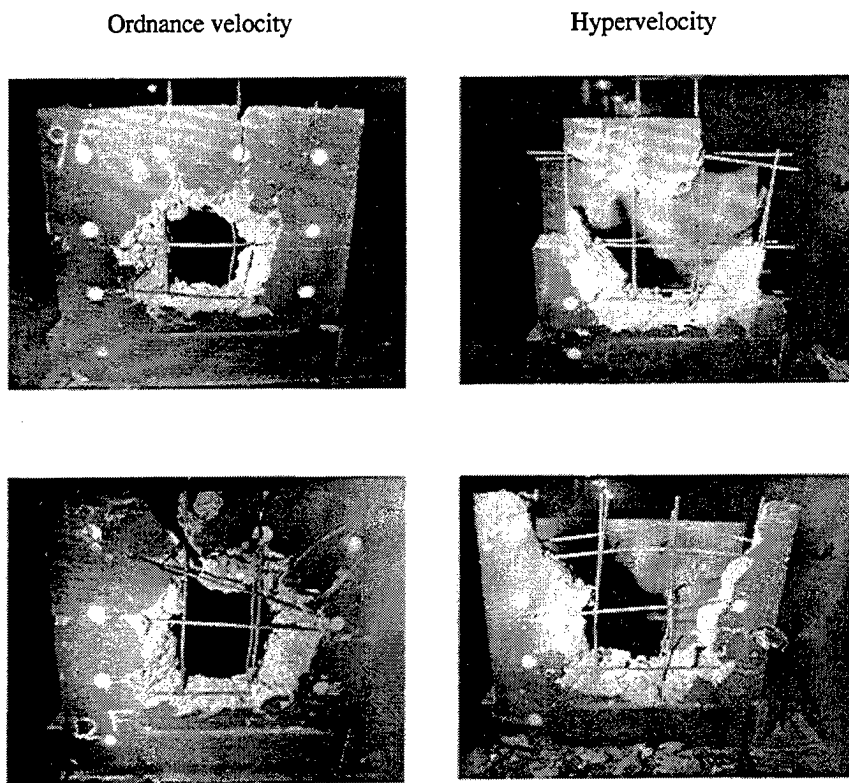


Figure 17. Illustration of Impacts for Equal Energies: 86 kJ (Top) and 100 kJ (Bottom).

One test was conducted with a concrete target containing no steel reinforcement. The velocity of the impact was $1,550\text{ m/s}$ and corresponded to a test where minor damage was observed in the DLRC target (14% mass loss). As expected, the nonreinforced concrete target suffered considerable damage (64% mass loss) when compared to the DLRC target with steel reinforcement.

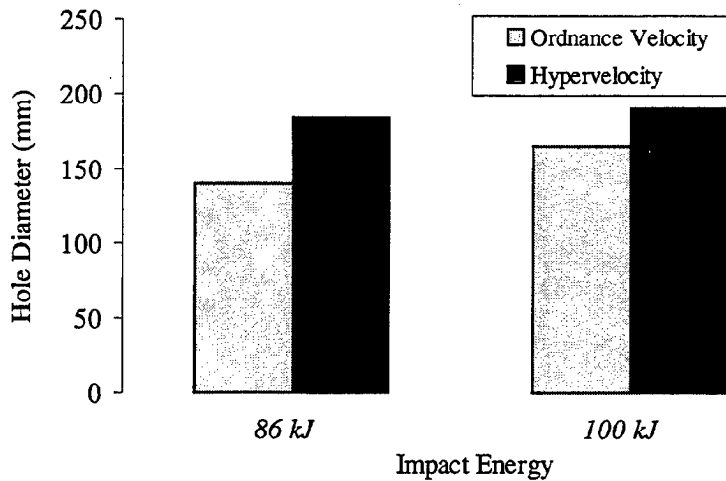


Figure 18. Hole Diameter for Equal Impact Energies.

Finally, another test was conducted where the slug, launched at a velocity of $1,211\text{ m/s}$, impacted the DLRC target at the location of the steel reinforcement bar. The hole created in the DLRC target was within 12% of the hole diameter created when the slug impacted a region absent of reinforcement and at a similar velocity. This data suggests that the damage is fairly insensitive to the location of the impact relative to the location of the steel reinforcement bar.

6. SUMMARY, CONCLUSIONS, AND RECOMMENDATIONS

Tests were conducted to assess the utility of hypervelocity impact of aluminum slugs into a DLRC target. The target was scaled from one that could be encountered in an urban environment. A 26-mm solid propellant gun was used to conduct the experiment. The calculated and measured values of gun system performance were in good agreement. Maximum case mouth pressure was 588 MPa (85 ksi) and produced a velocity of $2,223\text{ m/s}$ with a 58-g launch package.

Two slugs were considered: a 46-g and a 92-g slug. Impact results were compared for the 46-g slug as a function of impact velocity. Impacts were compared of the 92-g slug at equal striking energies. The diameter of the hole in the concrete target increased from 100 mm at an impact velocity of 1,178 m/s to the full lateral dimension of the target (450 mm) at 2,223 m/s. The residual penetration remained nearly constant as a function of impact velocity and was rather minor: scattered pits no deeper than 2 mm. The damage to the reinforcement in the target also increased from deformed (i.e., bent) at ordnance velocity to removed (one bar) at hypervelocity. The damage to the DLRC target was assessed by the amount of mass removed from the target, increasing from 10% of the initial 30-kg mass at ordnance velocity to 50% at hypervelocity.

Two tests were conducted with the 92-g slug corresponding to equal impact energies for the hypervelocity tests with the 46-g slug. In general, there was less damage to the concrete (smaller diameter hole and less mass removed) for the lower velocity tests. However, the residual penetration was significantly deeper (15 mm), suggesting a fair amount of residual penetrator length after perforating the DLRC target. There was considerably more debris generated behind the concrete target for the high-velocity tests than in the low-velocity tests.

The results suggest that there was increased damage to a reinforced concrete target by an impact from a hypervelocity slug as compared to an equal-energy slug at ordnance velocity. Although residual penetration was minimal with the shorter slug, further engineering and tests with a bimetallic slug may be able to balance terminal performance. Impacts at hypervelocity generated damage to the DLRC target that may be influenced by the finite lateral dimensions of the target. A larger target and/or smaller slug diameter may reduce this effect. Several tests, in which the target is exposed to an appropriate mass of HE, are needed to provide a comparison to the damage incurred from the kinetic energy impacts. Additionally, tests conducted at velocities greater than 2,300 m/s against more challenging targets may further demonstrate the utility of hypervelocity.

7. REFERENCES

1. Ellefsen, R., B. Coffland, and G. Orr. "Urban Building Characteristics: Setting and Structure of Building Types in Selected World Cities." NSWC/DL, TR-3714, Naval Surface Weapons Center, San Jose State University, San Jose, CA, January 1977.
2. Thein, B. K. and D. R. Coltharp. "Interim Standards for the Construction of MOBA Structures for Weapons Effects Tests." Technical Memorandum 30-78, U.S. Army Human Engineering Laboratory, Aberdeen Proving Ground, MD, December 1978.
3. Davis, J. Private communication. Waterways Experiment Station, Vicksburg, MS, September 1998.
4. Anderson, R., and K. Fickie. "IBHVG2 - A User's Guide." BRL-TR-829, U.S. Army Ballistic Research Laboratory, Aberdeen Proving Ground, MD, July 1987.
5. Devynck, D. Private communication. U.S. Army Research Laboratory, Aberdeen Proving Ground, MD, September 1998.

INTENTIONALLY LEFT BLANK.

Appendix:

Interior Ballistic Summary

INTENTIONALLY LEFT BLANK.

Table A-1. Interior Ballistic Summary.

37/26 mm, 10-ft Length Lab Gun								
M30 7-P, 0.022-in Web Propellant, MK22 MOD L70 Primer								
Shot ID	Aero Range Shot No.	Launch Mass	Insertion Force (a)	Charge Mass	No. Foam Wraps (b)	Muzzle Velocity	Peak Pressure (c)	Time to Peak (d)
		(g)	(kN)	(g)		(m/s)	(MPa)	(ms)
16	21655	57.9	3.98	125	2	1178	62	2.82
1	21640	57.9	0.99	125	2	1185	68	NM
15	21654	58.1	7.96	125	2	1211	68	2.28
6	21645	57.9	3.98	175	1	NR	146	1.74
13	21652	58.2	8.95	175	1	1548	176	1.83
2	21641	57.9	4.97	175	1	1553	137	1.84
3	21642	57.9	2.98	230	1	1905	344	1.68
7	21646	58.1	7.96	230	1	1942	NR	NR
5	21644	58.0	4.97	260	0	2119	NR	NR
8	21647	58.1	4.97	260	0	2143	498	1.17
4	21643	58.0	3.98	260	0	NR	495	1.34
12	21651	58.2	6.96	275	0	2224	591	1.12
9	21648	107.3	3.98	145	1	1213	113	2.21
10	21649	107.4	0.99	175	1	1392	205	2.11
11	21650	107.5	3.48	175	1	1388	209	2.30
14	21653	107.0	3.98	190	1	1462	268	1.67

Notes: NM = Not Measured.

NR = Not Recorded.

^a Use as shot-start pressure.

^b Used inside cartridge case, 3.8 mm thick.

^c Measured at case mouth.

^d From first perceptible rise.

INTENTIONALLY LEFT BLANK.

<u>NO. OF COPIES</u>	<u>ORGANIZATION</u>
2	DEFENSE TECHNICAL INFORMATION CENTER DTIC DDA 8725 JOHN J KINGMAN RD STE 0944 FT BELVOIR VA 22060-6218
1	HQDA DAMO FDQ D SCHMIDT 400 ARMY PENTAGON WASHINGTON DC 20310-0460
1	OSD OUSD(A&T)/ODDDR&E(R) R J TREW THE PENTAGON WASHINGTON DC 20301-7100
1	DPTY CG FOR RDE HQ US ARMY MATERIEL CMD AMCRD MG CALDWELL 5001 EISENHOWER AVE ALEXANDRIA VA 22333-0001
1	INST FOR ADVNCD TCHNLGY THE UNIV OF TEXAS AT AUSTIN PO BOX 202797 AUSTIN TX 78720-2797
1	DARPA B KASPAR 3701 N FAIRFAX DR ARLINGTON VA 22203-1714
1	NAVAL SURFACE WARFARE CTR CODE B07 J PENNELLA 17320 DAHLGREN RD BLDG 1470 RM 1101 DAHLGREN VA 22448-5100
1	US MILITARY ACADEMY MATH SCI CTR OF EXCELLENCE DEPT OF MATHEMATICAL SCI MAJ M D PHILLIPS THAYER HALL WEST POINT NY 10996-1786

<u>NO. OF COPIES</u>	<u>ORGANIZATION</u>
1	DIRECTOR US ARMY RESEARCH LAB AMSRL DD J J ROCCHIO 2800 POWDER MILL RD ADELPHI MD 20783-1145
1	DIRECTOR US ARMY RESEARCH LAB AMSRL CS AS (RECORDS MGMT) 2800 POWDER MILL RD ADELPHI MD 20783-1145
3	DIRECTOR US ARMY RESEARCH LAB AMSRL CI LL 2800 POWDER MILL RD ADELPHI MD 20783-1145
	<u>ABERDEEN PROVING GROUND</u>
4	DIR USARL AMSRL CI LP (305)

<u>NO. OF COPIES</u>	<u>ORGANIZATION</u>
1	DIR FOR THE DIRECTORATE OF FORCE DEVELOPMENT US ARMY ARMOR CENTER COL E BRYLA FT KNOX KY 40121-5000
1	US ARMY MATERIAL COMMAND AMC DCG T C KITCHENS 5001 EISENHOWER BLVD ALEXANDRIA VA 22333-0001
2	US ARMY RESEARCH LAB AMSRL C LE G MCNALLY 2800 POWDER MILL RD ADELPHI MD 20783-1145
1	DPTY ASST SEC FOR RD&A R CHAIT THE PENTAGON RM 3E480 WASHINGTON DC 20310-0103
1	US ARMY MISSILE COMMAND AMSMI RD DR MCCORKLE REDSTONE ARSENAL AL 35898-5240
1	WATERWAYS EXPERIMENT STATION SS E J DAVIS 3909 HALLS FERRY ROAD VICKSBURG MS 39180-6199
2	US ARMY TACOM TARDEC AMSTA TR D MS 207 J CHAPIN M TOURNER WARREN MI 48397-5000
1	US ARMY TACOM ARDEC AMSTA AR WEE C E BAKER BLDG 3022 PICATINNY ARSENAL NJ 07806-5000

<u>NO. OF COPIES</u>	<u>ORGANIZATION</u>
1	US ARMY TACOM ARDEC FSAE GCSS TMA J BENNETT BLDG 354 PICATINNY ARSENAL NJ 07806-5000
3	INST FOR ADVANCED TECH UNIV OF TEXAS AT AUSTIN P SULLIVAN F STEPHANI 4030 2 WEST BRAKER LANE AUSTIN TX 78759-5329
4	UNIV OF TEXAS AT AUSTIN CENTER FOR ELECT A WALLS J KITZMILLER S PRATAP PRC MAIL CODE R7000 AUSTIN TX 78712
1	LOCKHEED MARTIN VOUGHT R TAYLOR PO BOX 650003 MS WT 21 DALLAS TX 75265-0003
1	INST FOR DEFENSE ANALYSIS I KOHLBERG 1801 N BEAUREGARD ST ALEXANDRIA VA 22311
1	UNIV AT BUFFALO SUNY AB J SARJEANT PO BOX 601900 BUFFALO NY 14260-1900
2	UDLP B GOODELL R JOHNSON MS M170 4800 EAST RIVER RD MINNEAPOLIS MN 55421-1498

<u>NO. OF COPIES</u>	<u>ORGANIZATION</u>
1	UNIV OF TEXAS AT AUSTIN M DRIGA ENS 434 DEPT OF ECE MAIL CODE 60803 AUSTIN TX 78712
1	SAIC G CHRYSSOMALLIS 3800 WEST 80TH ST SUITE 1090 BLOOMINGTON MN 55431
1	SAIC J BATTEH 1225 JOHNSON FERRY RD SUITE 100 MARIETTA GA 30068
1	SAIC K A JAMISON 1247 B N EGLIN PKWY SHALIMAR FL 32579
2	IAP RESEARCH INC D BAUER J BARBER 2763 CULVER AVE DAYTON OH 45429-3723
3	MAXWELL TECHNOLOGIES J KEZERIAN P REIDY T WOLFE 9244 BALBOA AVENUE SAN DIEGO CA 92123
1	NORTH CAROLINA STATE UNIV M BOURHAM DEPT OF NUCLEAR ENGR BOX 7909 RALEIGH NC 27695-7909
1	MAXWELL PHYICS INTERNATIONAL C GILMAN 2700 MERCED STREET PO BOX 5010 SAN LEANDRO CA 94577-0599

<u>NO. OF COPIES</u>	<u>ORGANIZATION</u>
1	ATA ASSOCIATES W ISBELL PO BOX 6570 SANTA BARBARA CA 93160-6570
	<u>ABERDEEN PROVING GROUND</u>
26	DIR USARL AMSRL WM I MAY L JOHNSON AMSRL WM B A HORST E SCHMIDT AMSRL WM BE G WREN AMSRL WM BD B FORCH AMSRL WM BA W D'AMICO AMSRL WM BC P PLOSTINS D LYON J GARNER V OSKAY M BUNDY J SAHU P WEINACHT H EDGE B GUIDOS A ZIELINSKI D WEBB K SOENCKSEN S WILKERSON T ERLINE J NEWILL G COOPER AMSRL WM BE A BRANDT AMSRL WM TD G BOYCE AMSRL WM WD J POWELL

INTENTIONALLY LEFT BLANK.

USER EVALUATION SHEET/CHANGE OF ADDRESS

This Laboratory undertakes a continuing effort to improve the quality of the reports it publishes. Your comments/answers to the items/questions below will aid us in our efforts.

- 1. ARL Report Number/Author ARL-TR-2038 (Zielinski) Date of Report September 1999
- 2. Date Report Received _____
- 3. Does this report satisfy a need? (Comment on purpose, related project, or other area of interest for which the report will be used.) _____

- 4. Specifically, how is the report being used? (Information source, design data, procedure, source of ideas, etc.) _____

- 5. Has the information in this report led to any quantitative savings as far as man-hours or dollars saved, operating costs avoided, or efficiencies achieved, etc? If so, please elaborate. _____

- 6. General Comments. What do you think should be changed to improve future reports? (Indicate changes to organization, technical content, format, etc.) _____

CURRENT ADDRESS	_____
	Organization
	Name E-mail Name
	Street or P.O. Box No.

	City, State, Zip Code

7. If indicating a Change of Address or Address Correction, please provide the Current or Correct address above and the Old or Incorrect address below.

OLD ADDRESS	_____
	Organization
	Name
	Street or P.O. Box No.

	City, State, Zip Code

(Remove this sheet, fold as indicated, tape closed, and mail.)
(DO NOT STAPLE)